Substitution-induced superconductivity in $SrFe_{2-x}Ru_xAs_2$ ($0 \leq x \leq 2$)

W. Schnelle, A. Leithe-Jasper, R. Gumeniuk, U. Burkhardt, D. Kasinathan, and H. Rosner
Max-Planck-Institut für Chemische Physik fester Stoffe, Nöthnitzer Straße 40, 01187 Dresden, Germany
(Received 12 March 2009; revised manuscript received 6 May 2009; published 12 June 2009)

The magnetism in $SrFe_2As_2$ can be suppressed by electron doping through a small substitution of Fe by Co or Ni, giving way to superconductivity. We demonstrate that a massive substitution of Fe by isovalent ruthenium similarly suppresses the magnetic ordering in $SrFe_{2-x}Ru_xAs_2$ and leads to bulk superconductivity for $0.6 \leq x \leq 0.8$. Magnetization, electrical resistivity, and specific-heat data show T_c up to ≈ 20 K. Detailed structural investigations reveal a strong decrease in the lattice parameter ratio c/a with increasing x. Density functional theory band-structure calculations are in line with the observation that the magnetic order in $SrFe_{2-x}Ru_xAs_2$ is only destabilized for large x.

DOI: 10.1103/PhysRevB.79.214516 PACS number(s): 74.10.+v, 74.25.Bt, 74.25.Jb

I. INTRODUCTION

Soon after the discovery of superconductivity (SC) in doped *R*FeAsO (*R*=rare-earth element) materials,[1] investigations also focused on the structurally related AFe_2As_2 compounds (*A*=alkaline, alkaline-earth, or rare-earth metal). In the latter structures, the Fe_2As_2 slabs are separated only by single elemental *A* layers.[2] The compounds become superconductors if appropriately modified by substitutions on the *A* site by alkali metals[3–5] or direct substitution within the Fe_2As_2 slab by Co (Refs. 6–9) or Ni.[10] Recently, also the appearance of SC upon substitution of As by P was reported.[11] Controlled tuning of the electronic structure by selective substitutions provides an opportunity to test and refine theoretical models since these substitutions can introduce charge carriers, modify the lattice parameters, and may significantly suppress the structural/magnetic transitions observed in the ternary parent compounds.[2]

Application of external pressure has been understood as a "clean" alternative to substitutions in tuning the electronic state. AFe_2As_2 compounds indeed show crossover to SC at pressures as low as 0.4 GPa for $CaFe_2As_2$,[12–14] and high T_c were observed (27 K at 3 GPa for $SrFe_2As_2$; 29 K at 3.5 GPa for $BaFe_2As_2$).[15] Pressure reduces the antiferromagnetic (AFM) phase-transition temperature (T_0) in $SrFe_2As_2$ and an abrupt loss of resistivity hints for the onset of SC.[16–18] However, the nature of pressure (hydrostatic vs anisotropic strains) in these experimental procedures is currently up for debate.[19]

A feature common to both approaches (chemical substitution or external pressure) is the correlation of anisotropic changes in the crystal lattice with the suppression of the spin-density wave (SDW) type of AFM. Transition-metal (*T*) substitution studies in $AFe_{2-x}T_xAs_2$ carried out so far show a significant contraction of the tetragonal *c* axis length[6,7,10] and SC upon partial substitution of Fe by Co or Ni (electron doping) and an opposite trend if Fe is replaced with Mn (hole doping).[20] For the latter substitution series the SDW transition temperature T_0 is not suppressed with increasing x and no SC is observed.[20] In contrast, in indirectly doped $Sr_{1-x}K_xFe_2As_2$ and $Ba_{1-x}K_xFe_2As_2$ (Refs. 3–5) the *a* lattice parameter decreases with x while *c* increases, keeping the unit cell volume almost constant. For $BaFe_2As_{2-x}P_x$, an isovalent substitution where SC is observed for $x > 0.5$, both *a* and *c* decrease with x.[11] The fact that substitutions within the Fe_2As_2 slab with other *d* metals lead to superconductivity, albeit with lower T_c than for indirect doping, favors an itinerant electronic theory, in contrast to the strongly correlated cuprates.[6]

A point to note is that the modification of the electron count by substitutions is inevitably connected with structural changes in the Fe_2As_2 slabs. Unfortunately, for most substitution series only the unit cell dimensions are reported while further crystallographic data (bonding angles) are unknown. For pressure studies on $Sr/BaFe_2As_2$ compounds aiming at physical properties it is difficult to connect the results to variations in the crystal structure since corresponding compressibility studies are largely missing. Thus, currently, it is not known how the valence electron concentration *and/or* the structural parameters have to be modified by substitution in order to suppress the magnetism and eventually generate SC in AFe_2As_2 compounds.

Recently, Nath *et al.*[21] reported on the physical properties of $SrRu_2As_2$ and $BaRu_2As_2$, which are isostructural to $SrFe_2As_2$ and do not show SC.[22] On the other hand, the isostructural $LaRu_2P_2$ is a long-known superconductor with $T_c = 4.1$ K.[22] In this paper we present results of a study of the solid solution $SrFe_{2-x}Ru_xAs_2$. A massive substitution of Fe by nominally isoelectronic Ru suppresses the SDW-ordered state and bulk superconductivity is observed for $0.6 \leq x \leq 0.8$. Characterization of the SC state by magnetic susceptibility, electrical resistivity, and specific-heat measurements shows a maximum T_c of ≈ 20 K. Detailed crystallographic information of all samples of the series are obtained from full profile refinement of powder x-ray diffraction data (XRD). Band-structure calculations confirm that AFM order is only suppressed for *large* x, giving way to SC in $SrFe_{2-x}Ru_xAs_2$.

In this study we obtain the pertinent crystallographic details for a complete substitution series with magnetically ordered, superconducting, and normal-metallic ground states. Such data are a prerequisite for a future comparative study of substitution systems (with or without superconducting phases) based on the $SrFe_2As_2$ parent compound. Another aspect is that substitution with nominally isovalent Ru—in contrast to the supposed electron doping by Co or Ni—is expected not to change the charge. In this way also no charge

TABLE I. Crystallographic and electronic data for $SrFe_{2-x}Ru_xAs_2$: lattice parameters a, c, ratio c/a, cell volume V, refined [by WINCSD (Ref. 24)] positional parameter z of As, interatomic distance $d_{T\text{-As}}$, refined Ru content x, intensity (R_I) and profile (R_P) residuals, SDW (T_0) and superconducting transition temperature (T_c^{mag}; crossing of the tangent to the upper part of the field-cooled susceptibility transition with $\chi=0$) and from specific heat (T_c^{cal}; from two-fluid model fit, see text), idealized specific-heat jump $\Delta c_p/T_c^{cal}$, linear term γ to c_p, and Debye temperature calculated from β. T_c are only listed for bulk superconductors. fil.=observation of superconducting traces (filaments).

x nom.	a (Å)	c (Å)	c/a	V (Å^3)	z_{As}	$d_{T\text{-As}}$ (Å)	x ref.	R_I/R_P %	T_0 (K)	T_c^{mag} (K)	T_c^{cal} (K)	$\Delta c_p/T_c^{cal}$ (mJ/mol K^2)	γ	Θ_D (K)
0.0[a]	3.9243(1)	12.3644(1)	3.1507	190.5	0.3600(1)	2.388(1)	0		203					
0.1	3.93210(3)	12.3446(1)	3.1347	190.9	0.3603(1)	2.3911(3)	0.12	3.7/6.3	190					
0.2	3.94387(2)	12.2905(1)	3.1125	191.2	0.3602(1)	2.3922(3)	0.21	3.6/6.8	165					
0.3	3.95145(3)	12.2551(2)	3.1014	191.4	0.3601(1)	2.3924(4)	0.31	3.8/10.3	≈140					
0.4	3.96689(2)	12.1772(1)	3.0697	191.6	0.3599(1)	2.3925(4)	0.42	4.6/8.4	≈100	fil.				
0.5	3.97720(4)	12.1300(2)	3.0499	191.9	0.3597(1)	2.3927(5)	0.50	5.3/14.1		fil.	<2.0			
0.6	3.99178(2)	12.0635(1)	3.0221	192.2	0.3599(1)	2.3959(4)	0.61	4.2/7.8		19.3	19.8	13.4	6.2	232
0.7	4.00507(2)	12.0087(1)	2.9983	192.6	0.3598(1)	2.3976(3)	0.71	3.3/6.3		19.3	20.1	11.6	7.3	229
0.8	4.01096(2)	11.9835(1)	2.9877	192.8	0.3598(1)	2.3983(4)	0.81	4.9/7.5		17.6	17.2	13.6	6.7	231
1.0	4.04437(6)	11.8097(3)	2.9200	193.2	0.3597(1)	2.4015(5)	1.03	4.5/10.2		fil.	<2.0	0	6.9	243
1.5	4.09818(2)	11.5301(1)	2.8135	193.6	0.3593(1)	2.4056(4)	1.50	3.8/7.4						
2.0[b],[c]	4.16911(2)	11.1706(1)	2.6794	194.2	0.3591(1)	2.4148(4)	2	4.2/7.6					4.1[b]	270[b]

[a]From Ref. 25.
[b]$a=4.1713$ Å, $c=11.1845$ Å, and $V=194.6$ Å^3 (from Ref. 21).
[c]$a=4.168$ Å, $c=11.179$ Å, and $V=194.2$ Å^3 (from Ref. 22).

disorder is generated within the Fe_2As_2 slab. This is in contrast to substitutions with d metals from the cobalt or nickel group. On the other hand, Ru substitution possibly will generate disorder due to its heavier mass and larger size. Both scattering mechanisms seem to limit the achievable T_c of materials with in-plane substitutions, in contrast to SC material obtained through indirect doping of the Fe_2As_2 slabs by substitution on the A site.

II. EXPERIMENTAL AND CRYSTAL STRUCTURE

Samples were prepared by powder metallurgical techniques. Blended and compacted mixtures of precursor alloys SrAs and Fe_2As together with As and Ru powder were placed in glassy-carbon crucibles, welded into tantalum containers, and sealed into evacuated quartz tubes for heat treatment at 900 °C for 24 h to 7 d followed by several regrinding and densification steps. Samples were obtained in the form of sintered pellets. Details of powder XRD procedures and electron-probe microanalysis (EPMA) are given in previous publications.[6,20] The magnetic susceptibility was measured in a superconducting quantum interference device magnetometer (MPMS, Quantum Design) and the heat capacity by a relaxation method (MPMS, Quantum Design). The electrical resistivity was determined by a four-point dc method (current density <3 A mm^{-2}). Due to the contact geometry the absolute resistivity could be determined only with an inaccuracy of ±30%.

Band-structure calculations were performed within the local-density approximation (LDA) using the full potential local orbital code FPLO (version 8.00) with a k mesh of $24\times24\times24$ k points and the Perdew-Wang parametrization of the exchange-correlation potential. The used structural parameters were those from Table I.[23]

III. RESULTS AND DISCUSSION

For all samples the crystal structure of $ThCr_2Si_2$ type (space group $I4/mmm$) (Ref. 25) was refined from powder XRD data by full profile methods [Sr in $2a$ (0,0,0), Fe/Ru in $4d$ (0,1/2,1/4), and As in $4e$ $(0,0,z)$] (see Table I). In the powder x-ray diffractograms of samples with $x\geq0.5$ broadening of $(00l)$ reflections are observed suggesting some local disorder along [001]. Nevertheless, they give no evidence for superstructure formation due to long-range Ru ordering. The refined lattice parameters, the refined Ru occupancies, as well as EPMA unambiguously reveal the substitution of Fe by Ru. The nominal Ru contents are in good agreement with both the Ru occupancies from XRD and the EPMA data. The samples contained as minor impurity $Ru_{1-x}Fe_xAs$. Upon exchange of Fe by Ru a strong linear decrease in the c parameter of the unit cell is observed (−9.7% for $x=2$). The tetragonal a b plane and with it the transition-metal distance $d_{T\text{-}T}=a/\sqrt{2}$ expands by the substitution (by +6.2% for $x=2$). The increase in the distances $d_{T\text{-As}}$ with x on the other hand is small (+1.1% for $x=2$) and the z parameter of As decreases by only 0.25%. Surprisingly, the exchange of Fe by the larger Ru atoms[26] results only in a 2.0% increase in the unit cell volume V. The by far largest structural effect of Ru (or Co; Ref. 6) substitution is the strong decrease in the c/a ratio, i.e., a strong strainlike deformation with respect to the crystal lattice of the ternary Fe parent compound. Correspondingly, the tetrahedral bonding angles $\epsilon_{1,2}$ As-(Fe,Ru)-As depart from each other with increasing x. There are no visible discontinuous changes in these room-

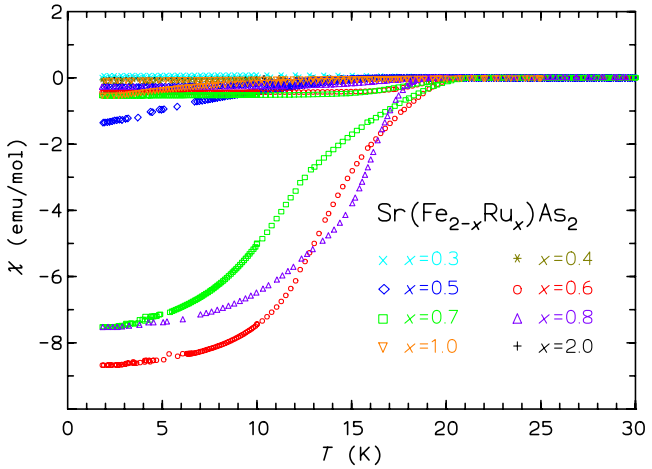

FIG. 1. (Color online) Magnetic susceptibility $\chi(T)$ of $SrFe_{2-x}Ru_xAs_2$ samples in a magnetic field $\mu_0 H=2$ mT.

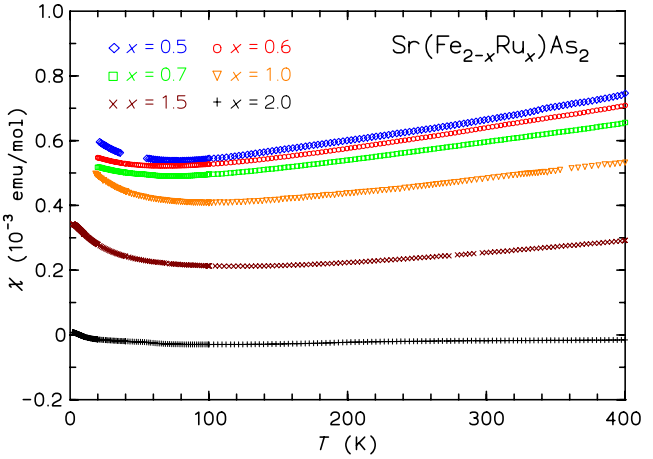

FIG. 2. (Color online) Corrected high-field magnetic susceptibility $\chi(T)$ of selected $SrFe_{2-x}Ru_xAs_2$ samples.

temperature structure data which could be connected to the various electronic ground states of $SrFe_{2-x}Ru_xAs_2$.

In Fig. 1 the low-field magnetic susceptibility of $Sr(Fe_{2-x}Ru_x)As_2$ samples is plotted. Weak diamagnetic signals for $T<16$ K in warming after zero-field cooling (ZFC) are already visible for a Ru concentration $x=0.4$. However, the diamagnetic shielding signal increases dramatically from $x=0.5$ to $x=0.6$. For $x=0.6$, 0.7, and 0.8 the shielding comprises the full volume of the sample suggesting bulk SC. On the other hand, the Meissner effect (measured during field cooling) is extremely small. This peculiarity is also observed for other $A(Fe_{2-x}T_x)As_2$ materials[6,7] and is probably due to strong pinning in materials with substitutions on the iron site, i.e., within the superconducting slab. The sample with $x=1.0$ also does not show bulk SC but only a very small diamagnetism after ZFC. The superconducting transition temperatures are listed in Table I; however, the transitions are rather broad. This observation of diamagnetic traces and the appearance of superconducting filaments for low Ru concentrations are certainly due to microscopic inhomogeneities of the Ru distribution.

The high-temperature susceptibility (high-field data eventually corrected for small ferromagnetic impurities, Fig. 2) of $SrFe_{2-x}Ru_xAs_2$ with $x\leq 1.5$ is generally paramagnetic and shows a typical linear increase with T for $T>100$ K, similar to that of compounds of the Co-substituted system.[6,27] The absolute values decrease systematically with the Ru content x as does the linear T dependence. $SrRu_2As_2$ finally is diamagnetic and shows no significant slope of $\chi(T)$ above 100 K, in agreement with Ref. 21. No phase transitions (except for SC) are observed for $x>0.5$. The samples with $x\leq 0.4$ display anomalies at around 200, 190, and 150–170 K for $x=0$, 0.1, and 0.2, respectively. These temperatures are close to the temperatures T_0 in Table I which were identified from the anomalies in the resistivity $\rho(T)$ (see below) which mark the SDW transition.

Due to the inaccuracy of the contact geometry we prefer to plot normalized electrical resistivity in Fig. 3. The room-temperature resistivity values $\rho(300\ \mathrm{K})$ are 500–800 $\mu\Omega$ cm for samples with $x=0$ and low Ru content x. The $\rho(300\ \mathrm{K})$ values decrease slightly with increasing x and for $SrRu_2As_2$ we find $\rho(300\ \mathrm{K})$ of only $\approx 230\ \mu\Omega$ cm. The temperature dependence of $\rho(T)/\rho(300\ \mathrm{K})$ corroborates the superconducting transitions. Zero resistivity is observed for Ru concentrations of $x=0.5$, 0.6, 0.7, and 0.8 at 7.0, 17.5, 16.0, and 18.0 K, respectively. The sample with $x=1.0$ also shows a drop in $\rho(T)$ below 18 K; however, $\rho=0$ is not reached at 4 K, indicating only filamentary SC. Also, a small drop in $\rho(T)$ at low T is already visible for $x=0.4$.

The resistivity of the sample $x=0.4$ however also shows a kink at $T_0\approx 100$ K, the $x=0.3$ sample at ≈ 140 K. For lower Ru concentration T_0 increases continuously (see Table I). The kink in $\rho(T)$, which roughly coincides with anomalies in the high-field susceptibility (see above), is the signature of the SDW transition[6,20,25,28] which is found at $T_0=203$ K in $SrFe_2As_2$.[25] Interestingly, in $Sr/BaFe_{2-x}Co_xAs_2$ crystals the resistivity for all $x>0$ increases below T_0 while for unsubstituted $Sr/BaFe_2As_2$, $\rho(T)$ decreases below T_0 (see, e.g., Refs. 6 and 29). In contrast, for $SrFe_{2-x}Ru_xAs_2$ the resistivity *decreases* below T_0 for all concentrations of Ru. Generally, for a full opening of a gap due to an SDW ordering an increase in $\rho(T)$ would be expected. Instead, it seems that the

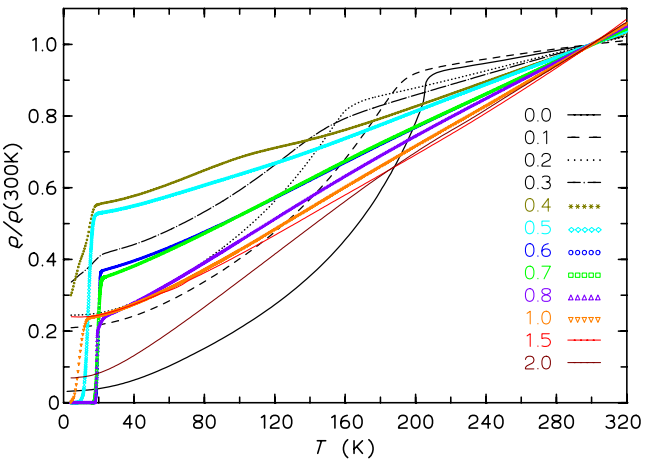

FIG. 3. (Color online) Electrical resistivity (normalized at 300 K) of $SrFe_{2-x}Ru_xAs_2$ samples (x as indicated on the curves). Data for $x=0$ from Ref. 28.

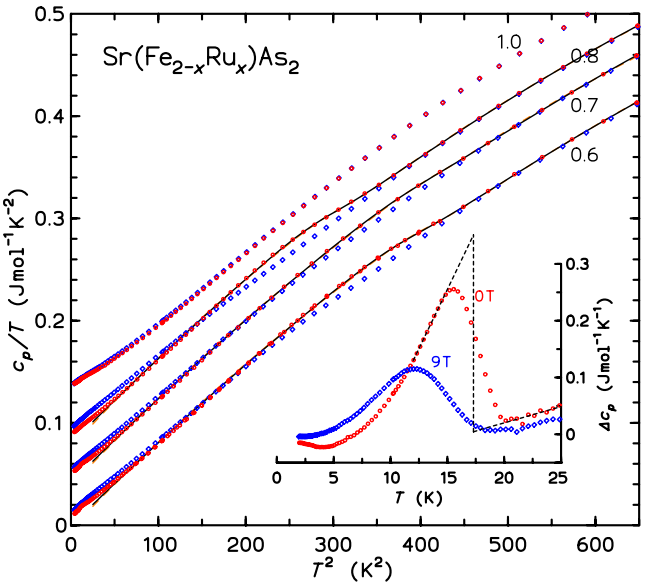

FIG. 4. (Color online) Specific heat c_p/T vs T^2 of $SrFe_{2-x}Ru_xAs_2$ (x=0.6, 0.7, 0.8, and 1.0). Data for zero magnetic field [circles (red)] are shown with the corresponding two-fluid [continuous curve (black)] and BCS [dashed curve (orange)]-type fits (see text). For a field $\mu_0 H$=9 T only data [diamonds (blue)] are shown. Data for x=0.7, 0.8, and 1.0 are shifted by 0.04, 0.08, and 0.12 units upward, respectively. Inset: difference of the specific heats (Δc_p) of the SC sample with x=0.8 and the sample x=1.0 (no bulk SC). Both the difference curves for 0 and 9 T fields are given. For the dashed lines construction, see the text.

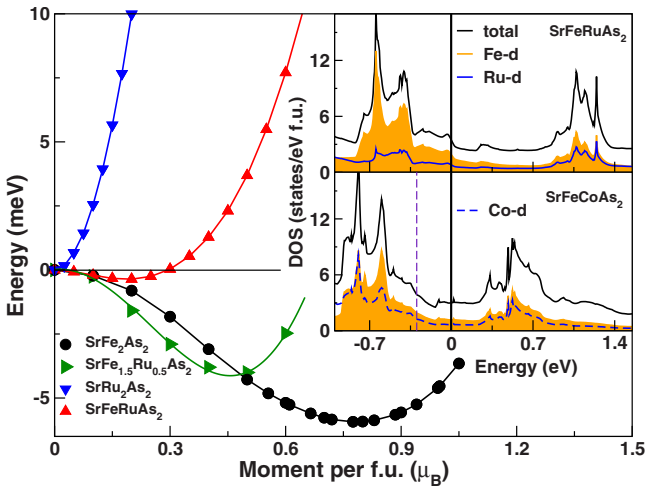

FIG. 5. (Color online) FSM curves for $SrFe_{2-x}Ru_xAs_2$ for x=0, 0.5, 1, and 2. The inset shows a comparison of the total and partial DOSs for $SrFeRuAs_2$ and $SrFeCoAs_2$. The dashed perpendicular line shows the Fermi level for $SrFe_2As_2$.

behavior of $\rho(T)$ below T_0 is connected to the presence or the absence of charge disorder caused by electron doping. Obviously, for $SrFe_{2-x}Ru_xAs_2$ and undoped materials, in the absence of such disorder, the mechanism leading to a decrease in $\rho(T)$ below T_0 is dominating.

The specific heat of selected samples is given in Fig. 4. Clear albeit broadened anomalies are seen close to the transition temperatures T_c^{mag} indicated by the low-field magnetization (see Table I). The sample with x=0.7 shows a less-pronounced transition than the samples with neighboring compositions. In agreement with the reduced resistive T_c, we conclude that this sample is inhomogeneous and of lower quality than the other samples. The sample with x=0.8 displays a pronounced transition at 17.2 K. The composition $SrFeRuAs_2$ shows no bulk SC above 2 K. Since the specific heats of the two latter samples are quite similar for $T \approx 20$ K the data for x=1 may serve as a reference for phonon and normal electronic contributions to the x=0.8 data. The inset in Fig. 4 shows the difference of the specific heat Δc_p of the samples. As can be seen for $T > T_c$, where Δc_p should be zero, the accuracy of this method is rather limited. Similar inaccuracies of Δc_p may be expected for $T < T_c$. We therefore refrain from fitting the temperature dependence of Δc_p and only estimate the size of the step $\Delta c_p/T_c$ at T_c by the usual entropy-conserving construction (shown schematically in Fig. 4 inset by the dashed lines). For H=0 we obtain 17.3(1) mJ mol^{-1} K^{-2} and T_c=17.3(5) K.

In order to obtain further electronic and phononic properties, the specific-heat data $c_p(T)$ between 5.0 and 25.5 K were fitted with a model including a phonon contribution (harmonic lattice approach $c_{\mathrm{ph}} = \beta T^3 + \delta T^5$) and an electronic term according to the weak-coupling BCS theory or the phenomenological two-fluid model. The latter model is a good approximation for the thermodynamic properties of some strong-coupling superconductors. Folding with a Gaussian simulates the broadening of the transitions due to chemical inhomogeneities. The parameters resulting from the fits are given in Table I. The relative specific-heat step $\Delta c_p/T_c$ at T_c^{cal} is quite similar for the three investigated SC samples. It has to be remarked that these values are smaller than the value obtained from the difference of the samples with x=0.8 and x=1.0. Nevertheless, the size of the specific-heat step at T_c is small and comparable to values observed for superconducting compositions of $SrFe_{2-x}Co_xAs_2$ (10–13 mJ mol^{-1} K^{-2}; hole doping within the Fe_2As_2 slab),[6] but much smaller than for, e.g., $Ba_{0.6}K_{0.4}Fe_2As_2$ ($\approx$98 mJ mol^{-1} K^{-2}).[30] The fits with the two-fluid models (shown in Fig. 4) are superior to those with the BCS model. The ratio $\Delta c_p/(\gamma T_c^{\mathrm{cal}})$ is $\approx$2.1, which is significantly larger than the weak-coupling BCS limit (1.43). Both these findings indicate strongly coupled SC, in agreement with μSR measurements (see, e.g., Ref. 31).

To understand the changes in the electronic structure upon substitution of Fe by Ru, we carried out band-structure calculations for x=0, 0.5, 1, and 2. The partial Ru substitution was modeled by supercells. Since any SDW pattern would be strongly influenced by the choice of the particular supercell, especially for the larger Ru content, we decided to compare the stability with respect to magnetism applying the fixed spin moment (FSM) approach (cf. Fig. 3 in Ref. 28). The resulting curves are shown in Fig. 5. As one may expect, the magnetic moment and the energy gain due to magnetic ordering are reduced with increasing Ru content x. The destabilization is especially strong between $0.5 \leq x \leq 1$; the fully Ru substituted compound is clearly nonmagnetic. In accord with the classical Stoner picture for itinerant magnets, the suppression of magnetism originates from a strong decrease

in the density of states (DOS) at the Fermi level $N(\varepsilon_F)=4.9$, 4.4, 3.5, and 1.9 states/(eV f.u.) for $x=0$, 0.5, 1, and 2, in agreement with experimental γ values (Table I).

In the real system the magnetism will be further destabilized due to the Fe-Ru disorder. In contrast to the Co-substituted compound, where the Co and Fe $3d$ states are almost indistinguishable (see inset of Fig. 5), the Ru $4d$ states differ considerably in the region close to ε_F. This difference has its origin in the different potential and lower site energy of Ru with respect to Fe. In turn, the distinct potential will be responsible for an enhanced scattering and therefore destabilize magnetic ordering. In the Co-substituted compound, however, only the shift in the Fermi level due to the additional electron (see Fig. 5) leads to a nonmagnetic state.

Although our calculation illustrates semiquantitatively the suppression of magnetism (clearing the scene for incipient SC) in $SrFe_{2-x}Ru_xAs_2$, the real interplay between magnetism and the slight volume expansion for increasing Ru content, accompanied by a reduction in the c axis and small changes in the As z position, is rather complex: the volume expansion leads to narrower Fe $3d$ bands that would stabilize magnetic order, but due to the c axis contraction these states are simultaneously shifted to lower energy resulting in a reduced DOS at ε_F. However, the Fe $3d$ states are pushed up in energy upon substitution of Ru due to the lower site energy of the Ru $4d$ states, compensating the reduction in $N(\varepsilon_F)$ partially. Furthermore, the Stoner factor I for Ru is significantly smaller than for Fe, disfavoring magnetic order further.

IV. DISCUSSION AND CONCLUSIONS

To summarize, we have shown that the partial isovalent substitution of Ru for Fe in $SrFe_2As_2$ suppresses the SDW transition and gives rise to bulk superconductivity. Both end members of the series, $SrFe_2As_2$ as well as $SrRu_2As_2$, crystallize in the $ThCr_2Si_2$-type structure ($I4/mmm$) and there is no indication of a change or of a superstructure for intermediate Ru concentrations at the applied experimental conditions. This observation indicates that Fe and Ru are isovalent. The lattice parameters a and c vary linearly but in opposite directions with x. As seen from the ratio c/a (decreases by 15% for x between 0 and 2) a strong anisotropic modification of the lattice (a compression of the tetragonal cell along c) is introduced by the exchange of Fe by Ru. While z_{As} does not change significantly with x, this implies a large change in the two different As-Fe-As bonding angles. While for $SrFe_2As_2$ these angles are quite similar (110.50° and 108.90°),[25] they deviate quite strongly in $SrRu_2As_2$ (119.43° and 104.73°). Bulk superconductivity exists in this series for a c/a ratio (at room temperature) around 3. Electronic properties such as the high-temperature susceptibility also show a smooth variation with x.

Whether any of these structural modifications is of special importance for the occurrence of superconductivity in $SrFe_{2-x}T_xAs_2$-type substitution series remains to be determined. Currently, it can be stated that electron doping by Co (or Ni) is much more efficient in order to suppress the SDW and allowing for a superconducting ground state than a compression of the cell along c. The fact that Ru substitutions do not suppress the SDW state for as low concentrations as for Co strongly indicates that Ru is isovalent to Fe in $SrFe_{2-x}Ru_xAs_2$. In (optimally superconducting) $SrFe_{1.80}Co_{0.20}As_2$ the c/a ratio is still quite large ($c/a=3.132$); however, 0.2 electrons were added per f.u.

In order to compare all these parameters further detailed structural studies on various $SrFe_{2-x}T_xAs_2$ systems are required. For the $BaFe_{2-x}(Co,Ni,Cu)_xAs_2$ systems a first attempt in this direction was presented recently.[32] Also, it is desirable to measure the compressibility of the compounds under hydrostatic pressure. Only such data would allow a comparison of pressure experiments with chemical substitution studies. During revision of this work, superconductivity in several systems $Sr/BaFe_{2-x}T_xAs_2$ with T=Ru,[33,34] Rh,[35] Pd,[36] and Ir (Ref. 37) was reported. For some of these systems the electronic state was already addressed by density functional theory methods.[38] Experimentally, it appears that the critical temperatures are generally limited to ≈20 K and that only for isovalent substitution (viz., Ru) the required level of substitution is such high as reported here. All these new $3d$, $4d$, and $5d$ metal substitutions deserve both an experimental as well as a sophisticated theoretical treatment, including the investigation of the influence of disorder and charge doping.

[1] Y. Kamihara, T. Watanabe, M. Hirano, and H. Hosono, J. Am. Chem. Soc. **130**, 3296 (2008).
[2] M. Rotter, M. Tegel, D. Johrendt, I. Schellenberg, W. Hermes, and R. Pöttgen, Phys. Rev. B **78**, 020503(R) (2008).
[3] M. Rotter, M. Tegel, and D. Johrendt, Phys. Rev. Lett. **101**, 107006 (2008).
[4] K. Sasmal, B. Lv, B. Lorenz, A. M. Guloy, F. Chen, Y. Y. Xue, and C. W. Chu, Phys. Rev. Lett. **101**, 107007 (2008).
[5] G. F. Chen, Z. Li, G. Li, W. Z. Hu, J. Dong, J. Zhou, X. D. Zhang, P. Zheng, N. L. Wang, and J. L. Luo, Chin. Phys. Lett. **25**, 3403 (2008).
[6] A. Leithe-Jasper, W. Schnelle, C. Geibel, and H. Rosner, Phys. Rev. Lett. **101**, 207004 (2008).
[7] A. S. Sefat, R. Jin, M. A. McGuire, B. C. Sales, D. J. Singh, and D. Mandrus, Phys. Rev. Lett. **101**, 117004 (2008).
[8] C. Wang, Y. K. Li, Z. W. Zhu, S. Jiang, X. Lin, Y. K. Luo, S. Chi, L. J. Li, Z. Ren, M. He, Y. T. Wang, Q. Tao, G. H. Cao, and Z. A. Xu, Phys. Rev. B **79**, 054521 (2009).
[9] N. Kumar, R. Nagalakshmi, R. Kulkarni, P. L. Paulose, A. K. Nigam, S. K. Dhar, and A. Thamizhavel, arXiv:0810.0848 (unpublished).
[10] L. J. Li, Q. B. Wang, Y. K. Luo, H. Chen, Q. Tao, Y. K. Li, X. Lin, M. He, Z. W. Zhu, G. H. Cao, and Z. A. Xu, New J. Phys. **11**, 025008 (2009).
[11] S. Jiang, C. Wang, Z. Ren, Y. Luo, G. Cao, and Z. Xu, arXiv:0901.3227 (unpublished).

[12] H. Lee, E. Park, T. Park, F. Ronning, E. D. Bauer, and J. D. Thompson, arXiv:0809.3550 (unpublished).
[13] T. Park, E. Park, H. Lee, T. Klimczuk, E. D. Bauer, F. Ronning, and J. D. Thompson, J. Phys.: Condens. Matter **20**, 322204 (2008).
[14] M. S. Torikachvili, S. L. Bud'ko, N. Ni, and P. C. Canfield, Phys. Rev. Lett. **101**, 057006 (2008).
[15] P. L. Alireza, Y. T. C. Ko, J. Gillett, C. M. Petrone, J. M. Cole, G. G. Lonzarich, and S. E. Sebastian, J. Phys.: Condens. Matter **21**, 012208 (2009).
[16] M. Kumar, M. Nicklas, A. Jesche, N. Caroca-Canales, M. Schmitt, M. Hanfland, D. Kasinathan, U. Schwarz, H. Rosner, and C. Geibel, Phys. Rev. B **78**, 184516 (2008).
[17] K. Igawa, H. Okada, H. Takahashi, S. Matsuishi, Y. Kamihara, M. Hirano, H. Hosono, K. Matsubayashi, and Y. Uwatoko, J. Phys. Soc. Jpn. **78**, 025001 (2009).
[18] M. S. Torikachvili, S. L. Bud'ko, N. Ni, and P. C. Canfield, Phys. Rev. B **78**, 104527 (2008).
[19] W. Yu, A. A. Aczel, T. J. Williams, S. L. Bud'ko, N. Ni, P. C. Canfield, and G. M. Luke, arXiv:0811.2554, Phys. Rev. B (to be published).
[20] D. Kasinathan, A. Ormeci, K. Koch, U. Burkhardt, W. Schnelle, A. Leithe-Jasper, and H. Rosner, New J. Phys. **11**, 025023 (2009).
[21] R. Nath, Y. Singh, and D. C. Johnston, arXiv:0901.4582 (unpublished).
[22] W. Jeitschko, R. Glaum, and L. Boonk, J. Solid State Chem. **69**, 93 (1987).
[23] For $SrFeCoAs_2$ the structural data of $SrFe_2As_2$ were used since Fe and Co are very similar in size.
[24] L. G. Akselrud, P. Y. Zavalii, Y. Grin, V. K. Pecharsky, B. Baumgartner, and E. Wölfel, Mater. Sci. Forum **133-136**, 335 (1993).
[25] M. Tegel, M. Rotter, V. Weiss, F. M. Schappacher, R. Pöttgen, and D. Johrendt, J. Phys.: Condens. Matter **20**, 452201 (2008).
[26] J. Emsley, *The Elements* (Clarendon, Oxford, 1992).
[27] X. F. Wang, T. Wu, G. Wu, R. H. Liu, H. Chen, Y. L. Xie, and X. H. Chen, New J. Phys. **11**, 045003 (2009).
[28] C. Krellner, N. Caroca-Canales, A. Jesche, H. Rosner, A. Ormeci, and C. Geibel, Phys. Rev. B **78**, 100504(R) (2008).
[29] K. Ahilan, F. L. Ning, T. Imai, A. S. Sefat, M. A. McGuire, B. C. Sales, and D. Mandrus, arXiv:0904.2215 (unpublished).
[30] G. Mu, H. Luo, Z. Wang, Z. Ren, L. Shan, C. Ren, and H. Wen, Phys. Rev. B **79**, 174501 (2009).
[31] R. Khasanov, A. Maisuradze, H. Maeter, A. Kwadrin, H. Luetkens, A. Amato, W. Schnelle, H. Rosner, A. Leithe-Jasper, and H. Klauss, arXiv:0903.1270 (unpublished).
[32] P. C. Canfield, S. L. Bud'ko, N. Ni, J. Q. Yan, and A. Kracher, arXiv:0904.3134 (unpublished).
[33] S. Paulraj, S. Sharma, A. Bharathi, A. T. Satya, S. Chandra, Y. Hariharan, and C. S. Sundar, arXiv:0902.2728 (unpublished).
[34] Y. Qi, L. Wang, Z. Gao, D. Wang, X. Zhang, and Y. Ma, arXiv:0903.4967 (unpublished).
[35] F. Han, X. Zhu, P. Chen, B. Shen, and H.-H. Wen, arXiv:0903.1028 (unpublished).
[36] X. Zhu, F. Han, and H.-H. Wen, arXiv:0903.0323 (unpublished).
[37] F. Han, X. Zhu, Y. Jia, L. Fang, P. Cheng, H. Luo, B. Shen, and H.-H. Wen, arXiv:0902.3957 (unpublished).
[38] L. Zhang and D. J. Singh, arXiv:0904.3984 (unpublished).